Task-Potency Investigations in Autism Spectrum Disorder

Tristan Looden[1], Roselyne Chauvin[1], Maarten Mennes[1], Jan Buitelaar[1,3], and Christian Beckmann[1,2]

[1]Donders Institute, Nijmegen
[2]FMRIB, Oxford
[3]Karakter, Nijmegen

Autism Spectrum Disorder (ASD) is a developmental disorder characterised by social and communicative deficits and repetitive behaviours. Research into ASD is challenged by heterogeneity among patients and a high prevalence of co-morbid disorders, such as Attention Deficit Hyperactivity Disorder (ADHD), a developmental disorder characterised by impulsivity, hyperactivity and/or inattention. Both ASD and ADHD are associated with functional brain alterations, observed in resting-state- and task-fMRI (functional magnetic resonance imaging) studies. To better characterise functional connectivity alterations related to performance on a specific task, we propose to use a measure called task-potency – which effectively enables comparing different tasks relative to a common baseline architecture, modelled from the resting state. In this study, we investigate whether modulation of connections during task performance is altered in ASD compared to control participants and whether different effects can be observed within the subpopulation of ASD meeting clinical criteria for ADHD. We observed that the ASD group employed greater modulation amplitude for each task. We further observed that the ASD_{ADHD+} (ASD subjects co-morbid with ADHD) group modulated fewer connections than TD (typically developing) when performing the Hariri and both reward tasks. Conversely, their mean modulation amplitude was greater than TD for every task. Moreover, we observed significant effects for ADHD symptom severity scores in the set of connections shared by the ASD_{TOTAL} (all ASD subjects) and ASD_{ADHD+} groups for Flanker, non-social reward and theory of mind tasks validating a co-morbidity effect. We found that task modulation amplitude in these five tasks is altered in ASD, but the participants without ADHD co-morbidity did not show this effect. Secondly, we found strong differences between ASD_{ADHD+} and TD in both the percentage of connections modulated as well as in the mean amplitude of modulation, and furthermore found effects of ADHD symptom severity on modulation amplitude for a set of connections in multiple tasks. We conclude that task-potency metrics display sensitivity to subgroup effects and therefore show potential for the development of stratification biomarkers.

Keywords: functional connectivity, fMRI, resting state, ASD, ADHD

Corresponding author: Tristan Looden; E-mail: t.looden@donders.ru.nl

Autism spectrum disorder (ASD) is a complex neurodevelopmental disorder marked by social and communicative deficits, as well as repetitive and restricted behaviors and interests. There appears to exist significant behavioral, cognitive and neural heterogeneity within ASD populations (Brunsdon & Happé, 2014; Nunes, Peatfield, Vakorin, & Doesburg, 2018). This has made investigations into any hypothetical underlying commonalities challenging. A further difficulty in ASD research lies where individuals diagnosed with ASD can also meet criteria for co-morbid disorders, most notably Attention Deficit Hyperactivity Disorder (ADHD) (Gargaro, Rinehart, Bradshaw, Tonge, & Sheppard, 2011). ADHD has itself been associated with functional brain alterations (Chauvin, Oldehinkel, Buitelaar, Beckmann, & Mennes, 2018) and it can be important to dissociate these alterations from those that might be related strictly to ASD. Attempts at describing ASD at a cognitive level have led to the emergence of several different theories (Hull et al., 2017). Relevant work has been published on how these various theories about ASD might interrelate at the cognitive level (Brunsdon & Happé, 2014). However, thus far our knowledge about how the neural processes that underlie tasks which tap into these cognitive domains interrelate is limited. The current research aims to advance our understanding of these cognitive interrelations in terms of their associated neural patterns in individuals with ASD and typically developing individuals through a method called 'task-potency'. Because this method incorporates both resting state and task-fMRI (functional magnetic resonance imaging) based measures of functional connectivity, we will start by briefly discussing resting state and task-fMRI functional connectivity findings in ASD before introducing the new angle of attack that task-potency allows us to take on.

Resting state functional connectivity in ASD

Analysis of resting-state fMRI data has proven to be a convenient means to ascertain functional connectivity patterns across brain areas. It provides insight into basal connectivity patterns, while at the same time being relatively easy to conduct independent of participant age and/or cognitive ability. The ASD resting state functional connectivity literature can roughly be divided into two classes of descriptions: broadly speaking that ASD brains exhibit either over-connectivity or under-connectivity relative to typically developing controls (Hull et al., 2017). The exact interpretation of these descriptions is, however, not trivial. For instance, what counts as over- or under-connectivity may be defined in several different ways. As an example, it can be defined globally (e.g., as an average value across all edges) or locally (e.g., as a value expressing the connectivity between one or several brain regions). Furthermore, the specific pattern of connectivity may be of relevance. For instance, a previous ASD study found diffuse over-connectivity with an aberrant pattern in ASD resting state fMRI data (Di Martino et al., 2011), whereas another resting state study found evidence for globally weaker connectivity, but also with an abnormal organisation (Yerys et al., 2017). Incongruent findings may further be driven by differences in factors such as age, sex and co-morbidity in the populations used, as well as the inherent heterogeneity present in ASD (Hull et al., 2017). These findings already underline the challenge of integrating results across studies and coming to a scientific consensus as to what might be going awry in the brains of individuals diagnosed with ASD. There is another layer of complexity to add in unravelling the neural underpinnings of cognition in ASD. Because even though resting state analyses provide a solid foundation of the functional architecture of the brain (Smith et al., 2009), it cannot tap into the processing underlying specific cognitive work. This means that task-based fMRI measures are crucial to include if the aim is to understand why deficits might be present in some cognitive domains but not so much in others, and where these dysfunctions present themselves.

Task-based functional connectivity in ASD

Task-based fMRI studies may be particularly useful in understanding abnormalities in ASD as they might more directly probe the neural correlates of the cognitive domains affected by the disorder. Studies using pattern recognition algorithms to predict ASD diagnoses from functional connectivity matrices derived from social reward tasks (Just, Cherkassky, Buchweitz, Keller, & Mitchell, 2014) and theory of mind tasks (Deshpande, Libero, Sreenivasan, Deshpande, & Kana, 2013) have reported substantial accuracy. The association of ASD with deficits in different cognitive domains has led to the inclusion of a varied battery of five tasks in the longitudinal European autism project in an attempt to probe a wide range of behavioural

and neural responses in participants (Charman et al., 2017a). However, as we know from the previous paragraph that complex findings have been reported at the level of the resting state, and because functional connectivity during tasks builds upon the ongoing activity architecture that resting state fMRI aims to estimate (Mennes et al., 2010), interpreting task-based functional connectivity findings is not straightforward. This study makes use of the novel task-potency method that provides a tool for disentangling the relative contribution of task-induced functional connectivity from that of the baseline architecture, potentially allowing a more precise interpretation of task-based functional connectivity findings and how these may vary across individuals and groups.

Task-potency

At its core, task-potency can be viewed as an analogue of the well-known fMRI activation designs in the realm of functional connectivity. Similar to where brain activation localization for a task is modelled with respect to a baseline condition, task-potency models the functional connectivity state that exists during a task with respect to the resting-state functional connectivity state. We consider the resting state a suitable baseline for the brain's functional architecture (Mennes et al., 2010). Through this modelling, we attain a new connectivity matrix which can be interpreted as the modulation away from the baseline - or 'potentiation', - that is instantiated in each edge due to engaging in the task, for any particular participant. The task potency framework then allows to isolate the task-based functional connectivity profile at a subject-specific level. In other words, for each subject and each task we attain a matrix of functional connectivity values across brain regions that represents the connectivity modulation away from the subject's resting state baseline that the cognitive demands in a particular task induce. This procedure can be repeated for a number of different tasks for each participant, where each task might have a particular way in which edges in the participant's brain are potentiated. Some tasks might potentiate a greater number of edges than others or potentiate a similar number of edges but with a greater amplitude. We might further investigate if there are edges that are potentiated above a certain threshold in many of the tasks under consideration and discover patterns therein. The tasks included in the current study intend to probe cognitive domains that are affected in ASD. We will apply the novel method of task-potency to analyse them and provide information about functional connectivity modulation in the ASD brain as compared to controls.

Materials and methods

Participants

The dataset from the EU-AIMS LEAP project was used for the current analyses (Charman et al., 2017). Data obtained from participants with intellectual impairments (IQ < 75) was excluded. Participants performed a resting state fMRI and one or more of the following task fMRI scans: Hariri emotion processing (Emotion) (Hariri, Tessitore, Mattay, Fera, & Weinberger, 2002), Flanker (inhibition) (Meyer-Lindenberg & Weinberger, 2006), non-social reward anticipation (Reward_ns), social reward anticipation (Reward_s) (Delmonte et al., 2012), animated shapes theory of mind (ToM) (Castelli, Frith, Happé, & Frith, 2002; White, Coniston, Rogers, & Frith, 2011). Additionally, each participant completed a T1-weighted anatomical scan for the purpose of registration. fMRI parameters are shown in the next paragraph. We further removed participants from the analysis for data quality using the following criteria. All participants had acceptable overlap (> 94%) with the MNI152 standard brain after image registration. We excluded 57 participants due to poor overlap (< 50%) with one or more regions from the brain parcellation atlas that had been chosen for the analysis (van Oort et al., 2017). Participants were further excluded on the basis of incidental findings, incomplete scans and those in the top 5% in terms of head motion quantified through RMS-FD (Jenkinson, Bannister, Brady, & Smith, 2002). The above criteria resulted in the inclusion of data for analyses from the following participants: 282 participants with autism spectrum disorder (age range: 7.5 - 30.3 years; M = 17.1; SD = 5.4; 72.3% male) and 221 typically developing controls (age range: 6.9 - 29.8 years; M = 17.0; SD = 5.5; 63.8% male) (see Fig. 1).

fMRI scanning parameters

MRI data were acquired on 3T scanners at multiple sites in Europe. Structural images were obtained using a 5.5 min MPRAGE sequence (TR = 2300 ms, TE = 2.93 ms, T1 = 900 ms, voxel size = 1.1 x 1.1 x 1.1 mm, flip angle = 9°, matrix size = 256 x 256, FOV = 270 mm, 176 slices). An 8 - 10 min

resting state fMRI (R-fMRI) scan was acquired using a multi-echo planar imaging (ME-EPI) sequence: TR = 2300 ms, TE = 12 ms, 31 ms, and 48 ms (slight variations are present across centers), flip angle = 80°, matrix size = 64 x 64, in-plane resolution = 3.8 mm, FOV = 240 mm, 33 axial slices, slice thickness/gap = 3.8 mm/0.4 mm, volumes = 200 (UMCU), 215 (KCL, CIMH) or 265 (RUNMC, UCAM). Participants were instructed to relax and fixate on a cross presented on the screen for the duration of the R-fMRI scan. The information was retrieved from Oldehinkel et al. (2019).

fMRI preprocessing

Preprocessing of the fMRI data was performed with tools from FSL 5.0.6. (Jenkinson, Beckmann, Behrens, Woolrich, & Smith, 2012). The first five volumes from each acquisition were removed to allow for equilibration of the magnetization. To correct for head movement, we performed volume realignment to the middle volume using MCFLIRT. This was followed by global 4D mean intensity normalization and smoothing with a 6 mm FWHM (full-width half maximum) kernel. ICA (independent component analysis)-aroma was used to identify and remove secondary motion-related artefacts (Pruim, Mennes, Buitelaar, & Beckmann, 2015; Pruim, Mennes, van Rooij, et al., 2015). Next, signal from white matter and CSF (cerebrospinal fluid) was regressed out and we applied a 0.01 Hz high-pass filter. For each participant, we registered acquisitions to their respective high-resolution T1 anatomical images by means of the Boundary-Based Registration (BBR) tool from FSL-FLIRT (Jenkinson et al., 2002). The high-resolution T1 image belonging to each participant was registered to MNI152 space with FLIRT 12 degrees-of-freedom linear registration and further refined using FNIRT non-linear registration (Andersson, Jenkinson, & Smith, 2007). We used the inverse of these transformations to take a brain atlas to the native space of each participant, where all further analyses were performed.

Behavioural data

We used clinical variables related to ASD and – in order to analyse possible co-morbidity effects – ADHD symptomatology in our analysis. For ASD, these were the total scores for the Social Responsiveness Scale Second Edition (SRS-2), the Repetitive Behaviours Scale - Revised (RBS-R) and the Short Sensory Profile (SSP). The SRS-2 contains questions about broad, characteristic ASD behaviours. The RBS-R contains questions specifically about repetitive and restrictive behaviours associated with ASD. The SSP scores abnormalities in sensory processing. For our analyses, we summed the SRS-2, RBS-R and SSP scores for each participant in order to produce an ASD symptom sum-score. For ADHD symptomatology, we used parent report scores for the clinical domains of inattentiveness and hyperactivity. We summed the ADHD hyperactivity and inattentiveness score for each participant in order to produce an ADHD symptom sum-score.

Task-potency calculation

We used a hierarchical brain atlas with 168 brain regions (distributed across 11 larger-scale networks) (van Oort et al., 2017) to superimpose on the native space of each subject and for each fMRI acquisition to define the regions. For each participant, we calculated the covariance between the average BOLD time series extracted from each brain region pair. Using Ledoit-Wolf regularization, we estimated partial correlations from the covariance matrix (Ledoit & Wolf, 2012) and consecutively applied the Fisher-Z transformation. This provided us with 168 x 168 connectivity matrices, one resting state matrix and one or more task matrices for each participant. The main Gaussian from a mixture Gaussian-gamma model, that was applied on each individual matrix, supplied us with parameterised information about the distribution of values in each matrix. We used these parameters to normalize the elements in each matrix. In order to produce individual matrices of connectivity modulations induced by the task (i.e., task-potency), we standardized each participant's task matrices by subtracting that participant's resting state matrix. The resulting matrices are interpreted as

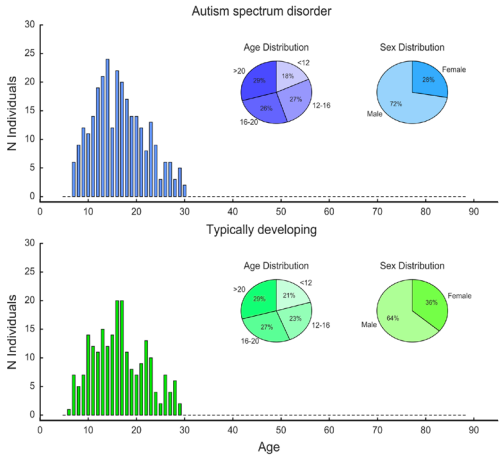

Figure 1. Demographical characteristics of the sample used in this study.

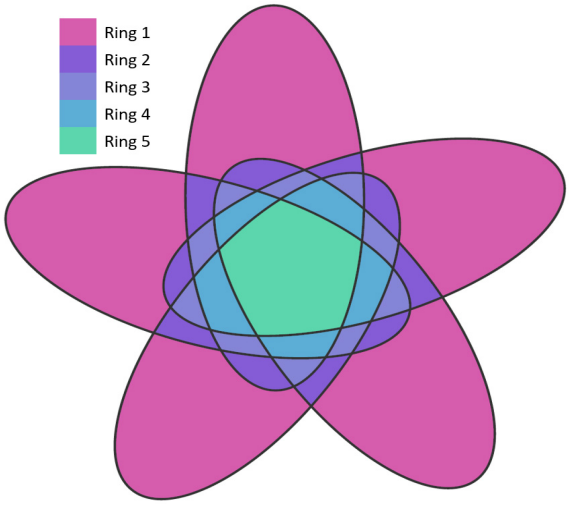

Figure 2. Venn diagram rings representation. Surface areas are not to scale. Each of the five overlapping ovals corresponds to the set of edges selected in one of the five tasks. The rings refer to those sets that are increasingly shared across multiple tasks with 'ring 5'at the centre, being the set that is shared across all of the tasks in the current paradigm

containing the connectivity modulations away from the resting state baseline that the respective task induces in the brain – we refer to these modulations as task-potency (Fig. 3) (Chauvin, Mennes, Llera, Buitelaar, & Beckmann, 2019).

Task-fingerprints

We obtained group-level task-potency matrices by averaging across participant potency matrices for each task within each participant group (ASD and TD). Within these group-level matrices, we identified the most strongly and consistently modulated edges by applying a threshold informed by a mixture modelling procedure (Bielczyk et al., 2018). The resulting binary matrices for each task and diagnostic group are referred to as task-fingerprints and consist of those edges sensitive to their respective task. We refer to the edges passing the threshold as 'selected edges' for that task. Within each diagnostic group, we now have five task-fingerprints, one per task. From these five fingerprint matrices, we can now identify those edges that are modulated by one particular task, as well as those edges that are modulated by two, three, four or all of the five tasks. Any edge can therefore be modulated by a combination of the five tasks, resulting in 32 (including the set of edges modulated by none of the tasks – the null set) possibilities across the tasks. We can report the proportion of edges modulated across tasks as a Venn diagram containing each of the 31 non-null sets of edges. To simplify our interpretation of these sets, we decided to define five categories as 'levels of modulation', which we can interpret as the level of generalization in the use of an edge. Essentially, we define five concentric 'rings' within the Venn-diagram representation, where each ring consists of all the sets that have the same sensitivity 'level'. For example, ring 1 consists of those five sets that are modulated in only one of the respective five tasks, and ring 5 consists of the one set that is modulated in each of the five tasks (Fig. 2). This representation allows us to make inferences about whether any connectivity differences, which we will test between ASD and TD, might be situated in for example a task-general or a task-specific domain.

Statistical testing

For ASD and TD, we investigated and compared edges that were selected in a particular task or in a particular ring. Four types of behaviour were investigated in the above conditions: 1) the percentage of selected edges, 2) the mean amplitude within the selected edges, 3) the normalized distribution of selected edges across the five sensitivity-levels, 4) the ratio of edges connecting areas within or between networks as defined in our atlas – across the five sensitivity-levels. For point 4, we average information across networks as we do not aim at investigating network-specific differences. Bootstrapping was used to provide a robust estimate of the variance within these measures. Here, 10000 samples were taken from the original data, each including a random 80% of participants of the groups involved, selected with replacement. This allowed us to produce an estimate of the uncertainty of the particular metric within the populations, which we need to quantify the uncertainty as to their difference. Any differences between ASD and TD in the obtained metrics above were then assessed using significance testing, where we assessed how surprising our findings were given the distributions that were obtained from the sample bootstrapping.

Results

Data

We had thus far obtained 2 (groups) x 5 (tasks) = 10 separate mean functional connectivity matrices which were thresholded to reveal the connectivity fingerprints, consisting of a selection of modulated edges for each of these ten groups. We compared

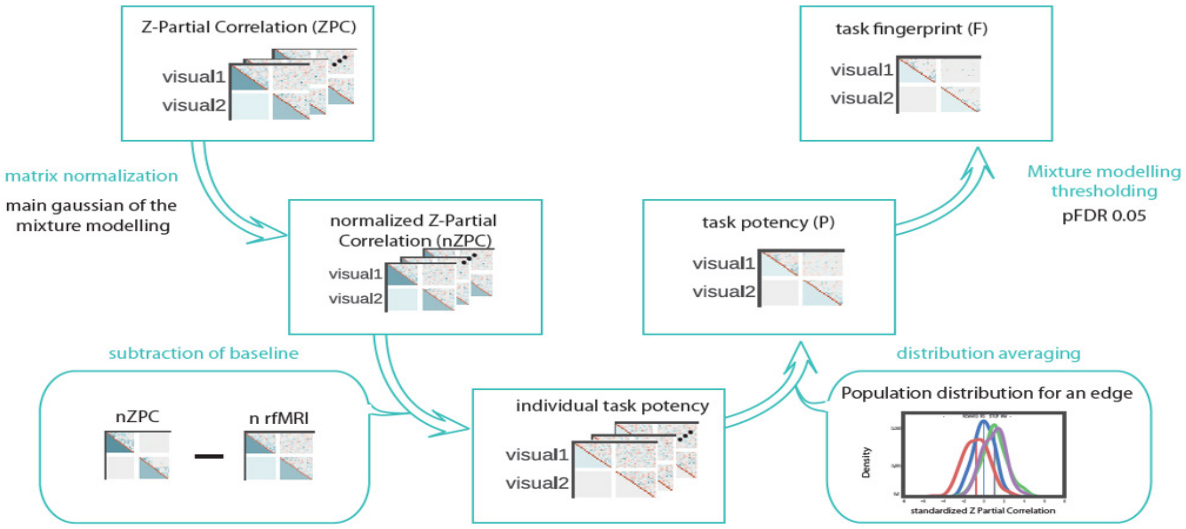

Figure 3. The task-potency pipeline.

the modulation strength, amount and spatial pattern of these selected edges between groups and tasks.

Comparisons between diagnostic groups

As the first step in analysing the data, we took the connectivity fingerprints and compared the amount of selected edges in each of these fingerprints between diagnostic categories for each task. Differences in the amount of selected edges present in the task connectivity fingerprint of diagnostic groups can provide insight into a global connectivity alteration where more or less edges are modulated to achieve the same task-goal. This could indicate more diffuse or more focused network involvement. In this measure, the specific spatial connectivity modulation profile (e.g., which networks connect where) was not taken into consideration. On first inspection, there appeared to be a trend for a greater amount of edges being recruited in performing the tasks in ASD as compared to TD across the tasks (Fig. 4). This could suggest a more diffuse modulation of edges across networks in ASD. However, the overall modulation across selected edges between groups was not significant in any of the five particular tasks (pairwise comparisons with FDR (false discovery rate) correction across tasks). Additionally, we noticed that different tasks modulated a different amount of edges in both diagnostic groups.

As a second step, we analysed the mean amplitude of modulation within the selected edges present in the fingerprints. For each diagnosis x task combination, we identified the mean amplitude of edge modulation across the edges (Fig. 4). After FDR correction across groups, we saw significant differences in the tasks Flanker ($p = 0.005$), social reward ($p = 0.001$), non-social reward ($p = 0.002$) and theory of mind ($p = 0.026$). In each of these tasks, the amplitude is lower for the ASD group, suggesting that the brain connectivity profile in the ASD group was not as strongly modulated in the

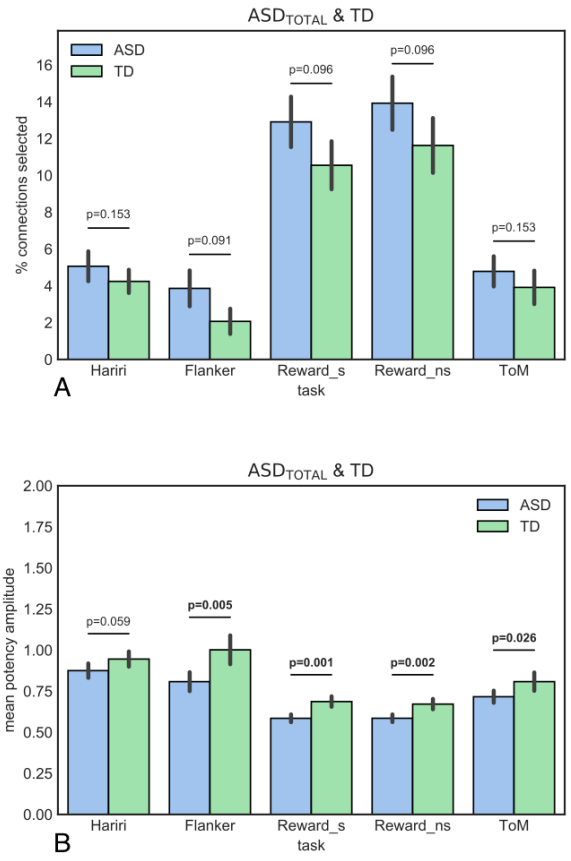

Figure 4. A. The percentage of edges that were consistently and strongly modulated in ASD_{TOTAL}. **B.** The mean potency amplitude of the selected edges in ASD_{TOTAL}.

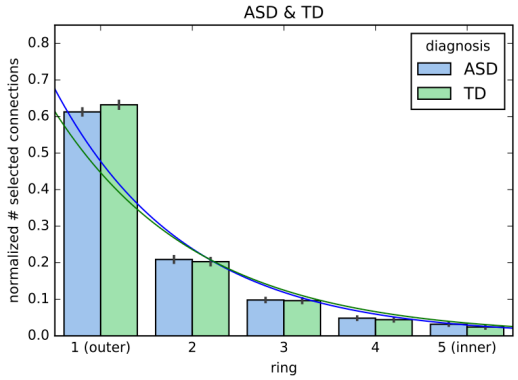

Figure 5. The distribution (normalized) of selected edges across the rings. Ring 1 contains only those edges selected in one task, while ring 5 contains those selected in all tasks.

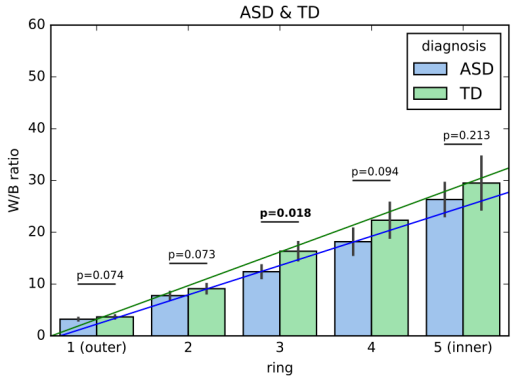

Figure 6. Displays the ratio of the amount of within-network edges to the amount of between-network edges in each ring set. Higher values correspond to greater within network connectivity. The lines indicate the linear fit for the respective diagnosis type of the of ring on the W/B ratio (β = 5.66, SD = 0.60 for ASD; β = 6.49, SD = 0.95 for TD).

face of any of these tasks as was the case for the TD group.

Comparisons between tasks

One of the primary goals of this investigation was to attempt to integrate brain connectivity findings across different tasks (i.e., cognitive domains) in the ASD population. As described earlier, for each task x group combination we obtain a task-fingerprint – containing those edges that passed our threshold for being consistently and strongly potentiated in their respective condition. If we consider these 'selected edges' for each of the tasks, we can represent edges that are modulated by one or a combination of tasks in a Venn-diagram. This allows us to describe similarity in terms of connectivity patterns between tasks. We focused our analysis on the level of selectivity across tasks, as in each edge being modulated by one, two, three, four or all five of the tasks (Fig. 2). The five areas defined as 'rings' within this diagram represent advancing levels of generalized modulation across tasks, with ring one being a combination of the five sets of edges that are only modulated in one specific task and ring five consisting of that set of edges which are modulated in each task. We investigated the way in which the amount of selected edges is distributed across these five rings and how this might differ between ASD and TD. For better visualization, the distributions were normalized within diagnosis group – meaning that the sum of the values across the five tasks, within diagnosis group, equals one. Because this makes the data dependent across rings, we modeled the representation of edges across the five rings using a parametric fit. We chose an exponential for this fit, based on visual inspection as well as for model simplicity. Using one fit per bootstrap, we extracted the distribution of the exponential coefficients for each group and compared if the representation of shared edges across rings shows a different pattern between the groups (Fig. 5). We find that the first parameter of the exponential fit is estimated as significantly greater in the ASD group ($p = 0.04$). This parameter indicates the intersect with the y-axis rather than the rate of decay, suggesting that the ASD group has a relatively greater proportion of edges that are specific to one task.

We had furthermore mapped the connectivity profile of each ring of edges, here defined as being edges that connect nodes either within or between networks. We quantified this per ring by taking the fraction of the amount of within-network edges and the amount of between network edges (W/B ratio). Higher values here correspond to greater within-network connectivity. Firstly, we observed that this ratio is always greater than one – replicating the finding that tasks preferentially modulate within network edges (Chauvin, Mennes, Buitelaar, & Beckmann, 2017). We further modeled a mean linear relationship between W/B ratio and the ring level using one fit per bootstrap (β = 5.66, SD = 0.60 for ASD, β = 6.49, SD = 0.95 for TD), where we found that edges shared by more tasks are increasingly more likely to be a within network edge. We did not find evidence of these linear effects differing between ASD and TD ($p = 0.14$). Visually, the TD group appears to recruit more within-network edges across each of the rings, however, this was only significant in ring 3 ($p = 0.018$) (FDR corrected across the five rings) (Fig. 6).

ASD and ADHD

In previous work, task-potency measures in an ADHD sample have displayed effects with a different direction than those found in the current study (Chauvin et al., 2018). It is further known that ASD and ADHD are frequently co-morbid. To investigate this possible confound, we separated our sample into 'ASD_{ADHD+}', consisting of those ASD subjects that met clinical classification cut-offs (DSM-5) for an unofficial ADHD diagnosis, and 'ASD_{ADHD-}', consisting of those subjects that did not meet the ADHD cut-off. In both cases, the cut off is defined as having a score of five or greater on either the hyperactivity or inattentiveness ADHD subscales as measured by parent-report. Out of our total sample of 282 ASD subjects, 201 fell into the ASD_{ADHD-} subgroup and 81 fell into the ASD_{ADHD+} subgroup. We remark that this means that some ADHD co-morbidity may be registered in almost 30% of the participants.

Potency profile of the different subgroups

In order to visualize any posited heterogeneity of the subgroups in relation to the total population with respect to their set of selected edges for each of the five tasks, we computed five Venn-diagrams (Fig. 7A). Inspecting the diagrams, we showed a number of trends occurring across the tasks: 1) Selection sizes appeared to be smaller for the subgroups than they are for the total. 2) The ASD_{ADHD-} and the ASD_{ADHD+} subpopulations appeared to cover large unique areas in the ASD_{TOTAL} (ASD_{ADHD-} and ASD_{ADHD+}) selected edges profile (yellow and purple areas in Fig. 7). 3) There was negligible overlap between the ASD_{ADHD-} and the ASD_{ADHD+} subpopulations outside of the ASD_{TOTAL} selected edges profile. In order to check whether effects might have been driven by co-morbid ADHD, we repeated the above analyses of Figure 4 in both the ASD_{ADHD-} and ASD_{ADHD+} subgroups. As the subgroups do not represent well-posed subpopulations, we only look for similarities or divergences in results compared to our original group.

Task-analysis in ASD_{ADHD-}

The amount of edges selected by the mixture model as showing strong connectivity modulation in each task appears lower, and hence more similar to TD, when we only use the ASD_{ADHD-} subgroup in the analysis (Fig. 8A). Just as was the case for the comparison for the selection of edges between the ASD_{TOTAL} group and TD, we do not find significant differences for a particular task. Furthermore, when we look at the amplitude present in these edges, we see that the values for the ASD_{ADHD-} subgroup appear closer to normal TD values (Fig. 8B). None of the current comparisons exceed the significance threshold for differences.

Task-analysis in ASD_{ADHD+}

We find that the ASD_{ADHD+} group as a whole recruits significantly more edges due to task demands compared to TD in all but the Flanker task (Fig. 9A). Moreover, inspecting the mean potency amplitude of these edges shows us that the potentiation taking place is more powerful in the ASD_{ADHD+} group compared to TD for all the tasks (Fig. 9B).

Modelling potency from symptom scores in ASD and ADHD

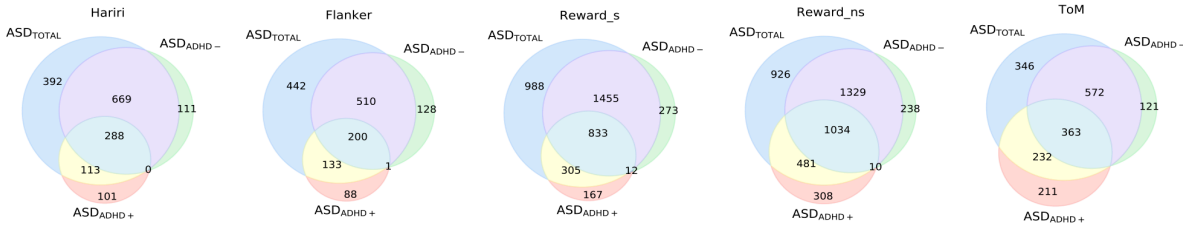

	ASD score	ADHD score		ASD score	ADHD score		ASD score	ADHD score		ASD score	ADHD score		ASD score	ADHD score
Potency	0.65	0.79	Potency	0.99	0.34	Potency	0.89	0.99	Potency	0.80	0.34	Potency	0.56	0.98
Potency	0.52	0.34	Potency	0.99	**0.02**	Potency	0.52	0.34	Potency	0.99	0.07	Potency	0.34	0.19
Potency	0.34	0.09	Potency	0.98	**<0.01**	Potency	0.56	0.07	Potency	0.98	**<0.01**	Potency	0.33	**0.02**

Figure 7. Venn diagrams displaying percentage of shared and unique modulated edges for the ASD_{TOTAL} group and its two subgroups, ASD_{ADHD-} and ASD_{ADHD+}. The numbers denote the amount of modulated edges in each Venn-set. The table shows significance values for a linear model predicting the mean potency amplitude of edges within the respective Venn-set from ASD and ADHD symptom scores and age.

As a way of investigating whether we can link potency to ASD and ADHD severity, we model the mean potency amplitude of the edges in the respective sets from ASD and ADHD aggregate symptom scores (Fig. 7B). Interestingly, for the Flanker, non-social reward and theory of mind tasks, we find significant positive associations between ADHD symptom scores and the set of edges that was selected in both the ASD_{TOTAL} and ASD_{ADHD+} groups but not the ASD_{ADHD-} group (yellow area in Fig. 7). We furthermore find a significant positive association between ADHD scores and the set of edges selected in all three conditions for the Flanker task. We do not find significant associations between ASD symptom scores and a particular set of edges in any of the current tasks. All significance values are FDR corrected for the 15 possible set x task combinations.

Discussion

Theories on ASD, such as weak central coherence and excitation/inhibition imbalance, suggest pervasive, global alterations in brain connectivity (Hull et al., 2017). For this reason, we have focused our first inquiry on general alterations in the way brain connectivity is modulated in the previously mentioned five tasks. When we compared the percentage of modulated edges away from the baseline architecture of the brain in the overall ASD group (ASD_{TOTAL}) to the TD group, we found no significant differences. However, when we measure the amplitude of modulation, we find that it is lower in the $ASDT_{OTAL}$ group for four of the five tasks under consideration (flanker, social reward, non-social reward, theory of mind). This could mean that even though participants with ASD engage a normal percentage of their connectome in performing

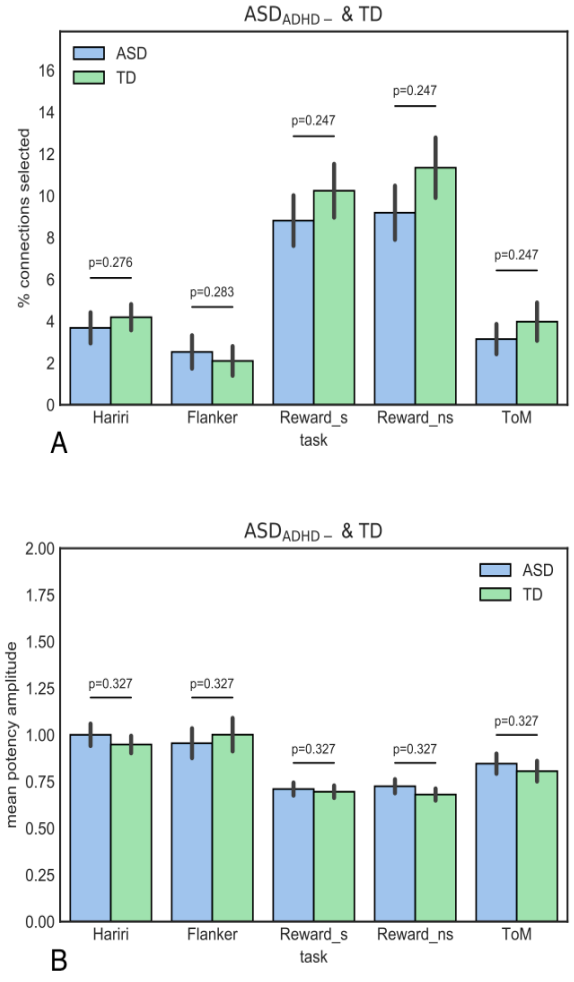

Figure 8A. The percentage of edges that were consistently and strongly modulated in ASD_{ADHD-}. B. The mean potency amplitude of the selected edges in ASD_{ADHD-}.

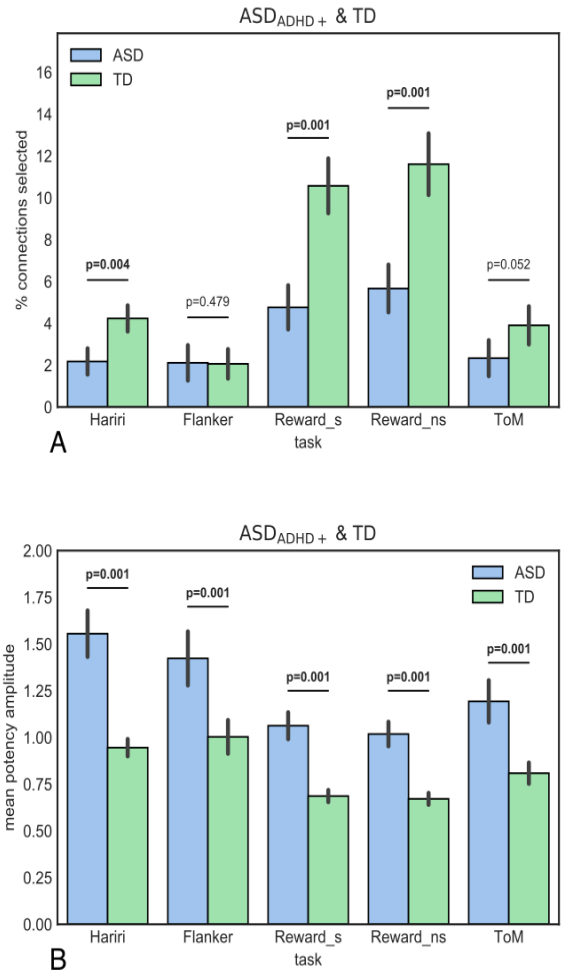

Figure 9A. The percentage of edges that were consistently and strongly modulated in ASD_{ADHD+}. B. The mean potency amplitude of the selected edges in ASD_{ADHD+}.

a task, the altered strength of these modulations could be a reason for their impairments in achieving the respective cognitive goals. We did not find this alteration for the Hariri emotion processing task, suggesting that the lower modulation present in ASD may be specific to certain tasks. Or rather to a cognitive process underlying the above tasks, but not emotion processing. In other words, the task profiles (i.e., which edges are potentiated for a particular task) are similar between ASD and TD, but not the amplitude of their modulation. It is important to reiterate is that the effect of individual differences in base resting state connectivity architecture is explicitly removed from the analyses in this paper. As such, if we do not find differences in task modulation, we might hypothesise that the connectivity alteration previously observed in the resting state (Hull et al., 2017) could be a core alteration influencing the integration of overall information during task performance.

As the tasks involved in this study have been selected for their implication in ASD (Charman et al., 2017), finding altered connectivity in a set of edges common to these tasks could help us in searching for the brain processes at the root of ASD symptoms. This approach was used because it might help us to identify whether any alterations are primarily found in those edges that are specific to certain tasks or rather in edges that are involved in multiple or all the tasks. In order to explore similarities and differences between task modulation profiles, as well as how these might differ between groups, we constructed a Venn-diagram of the sets of edges (task profile) involved in each of the five current tasks. We found for both groups that the majority of edges across the five tasks are task specific, with fewer edges modulated across tasks as we go towards considering sets selected in higher numbers of tasks (i.e., each consecutive ring). Very few edges were common across all five tasks. In order to find out whether this pattern differed between the groups, we modelled this 'decay' from specific to common edges for both groups with an exponential curve. We found that the model showed some difference in the initial state but importantly no difference in the rate of decay, providing no evidence that the task profile in ASD is altered. This contrasts for instance with what has been found for ADHD (Chauvin et al., 2018), where a lack of common processing compared to TD has been identified.

The weak central coherence theory of autism refers to the apparent cognitive deficits individuals with ASD have with fluently integrating/segregating information (e.g., 'not seeing the forest for the trees') (Brunsdon & Happé, 2014). If we make the biologically plausible assumption that adjacent types of information processing occur in adjacent brain regions, this allows us to investigate this cognitive theory aided by fMRI data. Adjacency can be defined, for instance, in terms of graph theoretical distance or Euclidean distance. Indeed, previous evidence in line with the weak central coherence hypothesis of ASD suggests that there may be resting state underconnectivity at short range and overconnectivity at long range in the ASD brain (Happé & Frith, 2006; Hull et al., 2017). Adjacency can, however, also be defined in functional terms (e.g., as resting state networks). The task-potency method allowed us to assess whether such a pattern can also be observed when it comes to the connectivity modulation that occurs during a task. Because we make use of a hierarchical atlas (11 large-scale networks, in which 168 smaller-scale areas are situated), we have the ability to classify edges as being either within or between networks, which served as our measure for adjacency of processing. We found that edges in both groups become more likely to be within-network edges as we look at the sets that are selected in more tasks. In other words, processing that is more general and shared across multiple cognitive domains is much more likely to take place within the same networks when compared to processing that is only implicated in a single task. Contrary to the literature that has associated ASD with short range overconnectivity, we have not found evidence for this in our analyses. We rather find that in ring 3, the TD group has significantly greater within-network oriented edges. We can hypothesise that only observing an effect in ring 3 might be due to a particular interaction between three of the tasks, which fall under this umbrella. More investigation is needed by selecting specific tasks together, as we cannot compare our results to the existing literature on short- and long-range connectivity. Indeed, we analysed modulation of connectivity during tasks rather than resting- state connectivity and we cannot compute the distance in terms of graph theoretical metrics as we focused on a subset of edges modulated during the task and removed the underlying architecture that connects them.

In order to investigate variability and heterogeneity in our ASD sample and because previous findings have shown that the task profile is altered in ADHD (Chauvin et al., 2018), we decided to compare the task profiles of an ASD group, which also scored high on ADHD symptoms, to

the rest of the ASD sample. Because of the high levels of ADHD co-morbidities known to exist in ASD cohorts, we were able to split the ASD group up into two groups, ASD_{ADHD-} and ASD_{ADHD+} with respectable sizes. In the ASD_{ADHD-} group, where participants with ADHD were excluded, we did not find any effect for either percentage of modulated edges or their amplitude. This might suggest that the amplitude effect, that was found in the original ASD_{TOTAL} group, could have been in fact driven by the subjects with ADHD. Though we find a significant amplitude effect in ASD_{ADHD+} for each of the tasks, they have an opposite direction to the effects found for ASD_{TOTAL}, with the ASD_{ADHD+} group rather having greater modulation amplitudes than TD. The fact that the amplitude findings of ASD_{TOTAL} are not a simple weighted average of ASD_{ADHD+} and ASD_{ADHD-} implies that these groups must have had differences in the set of edges from which this amplitude was calculated. This led us to computing the selected edges for each of the five tasks for these new groups and we found that they mostly make use of different sets of edges to perform tasks. What appeared to be a confound due to heterogeneity in the population now suggests that our method is highly sensitive to group differences even if they come from subgroups. Further research is needed to investigate how this generalises to other ways of splitting populations and whether it can be used to correctly classify individual participants. For example, we can try to assess whether observed differences are characteristics of the entire population by using this as input in a normative modelling analysis (Marquand, Wolfers, Mennes, Buitelaar, & Beckmann, 2016). In this approach, participants' deviance from a norm defined in the sample is assessed in order to capture subgroup effects or even individual profiles.

We found a significant positive association of ADHD symptom scores and mean potency amplitude in the Flanker, non-social reward and theory of mind tasks. This was the case when we considered a set of selected edges that was common between ASD_{TOTAL} and ASD_{ADHD+} but not ASD_{ADHD-}. These particular tasks have a strong executive function component, which is known to be impaired in ADHD (Gargaro et al., 2011). This finding may form a steppingstone to a possible clinical/diagnostic application of task-potency in ADHD. Further research can be done in a cohort of ADHD participants to narrow down which edges are responsible for driving this effect and to find out whether we have identified an ADHD-related effect or rather an ASD-ADHD co-morbidity effect.

In the current research, we take a holistic perspective at brain connectivity modulation. We analyse characteristics of the sets of selected edges independently of their spatial localisation, taking a general view on whole brain connectivity. Even when investigating edges as being within or between networks, where we carry out a slightly finer grained analysis, we still aggregate across tasks and loose some resolution in that dimension. It stands to reason that there may exist many relevant differences between (and within) the groups under consideration with respect to task-potency that we have not detected, which are left to future research. As it is known that ASD has a component of sensory processing abnormalities, it could for instance be interesting to compare and contrast the task profiles of sensory versus higher-order regions.

In summary, we found that participants with ASD less strongly modulate those parts of their functional connectome that are involved in tasks. However, splitting the ASD group with respect to ADHD co-morbidity, we find that for ASD_{ADHD-} these effects disappear whereas for ASD_{ADHD+} we find strong differences in their task profile compared to controls. We furthermore found that as edges are involved in performing multiple tasks, they are proportionally more likely to be within network edges. Lastly, we related ADHD symptom scores to mean potency amplitude in a set of edges but were not able to do the same for ASD symptom scores. We have shown that task-potency is a method of integrating task fMRI data which shows promise in the domains of parsing heterogeneous clinical groups as well as predicting symptom scores from fMRI data.

References

Andersson, J. L. R., Jenkinson, M., & Smith, S. (2007). Non-linear registration, aka spatial normalisation. FMRIB Technial Report TR07JA2. Oxford Centre for Functional Magnetic Resonance Imaging of the Brain, Department of Clinical Neurology, Oxford University, Oxford, UK(June), 22.

Bielczyk, N. Z., Walocha, F., Ebel, P. W., Haak, K. V., Llera, A., Buitelaar, J. K., ... & Beckmann, C. F. (2018). Thresholding functional connectomes by means of mixture modeling. NeuroImage.

Brunsdon, V. E., & Happé, F. (2014). Exploring the 'fractionation' of autism at the cognitive level. Autism, 18(1), 17–30.

Castelli, F., Frith, C., Happé, F., & Frith, U. (2002). Autism, Asperger syndrome and brain mechanisms for the

attribution of mental states to animated shapes. Brain: a journal of neurology, 125(8), 1839–1849.

Charman, T., Loth, E., Tillmann, J., Crawley, D., Wooldridge, C., Goyard, D., ... & Buitelaar, J. K. (2017a). The EU-AIMS Longitudinal European Autism Project (LEAP): Clinical characterisation. Molecular Autism, 8(1), 1–21.

Charman, T., Loth, E., Tillmann, J., Crawley, D., Wooldridge, C., Goyard, D., ... & Buitelaar, J. K. (2017b). The EU-AIMS Longitudinal European Autism Project (LEAP): Methods. Molecular Autism, 8(1), 1–19.

Chauvin, R., Oldehinkel, M., Buitelaar, J. K., Beckmann, C. F., & Mennes, M. (2018). Inefficient use of the brain' s functional infrastructure in ADHD Abstract. bioRxiv.

Chauvin, R. J., Mennes, M., Buitelaar, J. K., & Beckmann, C. F. (2017). Assessing age-dependent multi-task functional co-activation changes using measures of task-potency. Developmental Cognitive Neuroscience (March), 0–1.

Chauvin, R. J., Mennes, M., Llera, A., Buitelaar, J. K., & Beckmann, C. F. (2019). Disentangling common from specific processing across tasks using task potency. NeuroImage, 184(September 2018), 632–645.

Delmonte, S., Balsters, J. H., McGrath, J., Fitzgerald, J., Brennan, S., Fagan, A. J., & Gallagher, L. (2012). Social and monetary reward processing in autism spectrum disorders. Molecular Autism, 3(1), 1–13.

Deshpande, G., Libero, L. E., Sreenivasan, K. R., Deshpande, H. D., & Kana, R. K. (2013). Identification of neural connectivity signatures of autism using machine learning. Frontiers in Human Neuroscience, 7(October), 1–15.

Di Martino, A., Kelly, C., Grzadzinski, R., Zuo, X. N., Mennes, M., Mairena, M. A., ... & Milham, M. P. (2011). Aberrant striatal functional connectivity in children with autism. Biological Psychiatry, 69(9), 847–856.

Gargaro, B. A., Rinehart, N. J., Bradshaw, J. L., Tonge, B. J., & Sheppard, D. M. (2011). Autism and ADHD: How far have we come in the comorbidity debate? Neuroscience and Biobehavioral Reviews, 35(5), 1081–1088.

Happé, F., & Frith, U. (2006). The weak coherence account: Detail-focused cognitive style in autism spectrum disorders. Journal of Autism and Developmental Disorders, 36(1), 5–25.

Hariri, A. R., Tessitore, A., Mattay, V. S., Fera, F., & Weinberger, D. R. (2002). The amygdala response to emotional stimuli: A comparison of faces and scenes. NeuroImage, 17(1), 317–323.

Hull, J. V., Jacokes, Z. J., Torgerson, C. M., Irimia, A., Van Horn, J. D., Aylward, E., ... & Webb, S. J. (2017). Resting-state functional connectivity in autism spectrum disorders: A review. Frontiers in Psychiatry, 7(JAN).

Jenkinson, M., Bannister, P., Brady, M., & Smith, S. (2002). Improved optimization for the robust and accurate linear registration and motion correction of brain images. NeuroImage, 17(2), 825–841.

Jenkinson, M., Beckmann, C. F., Behrens, T. E. J., Woolrich, M. W., & Smith, S. M. (2012). FSL. NeuroImage, 62(2), 782–790.

Just, M. A., Cherkassky, V. L., Buchweitz, A., Keller, T. A., & Mitchell, T. M. (2014). Identifying autism from neural representations of social interactions: Neurocognitive markers of autism. PLoS ONE, 9(12), 1–22.

Ledoit, O., & Wolf, M. (2012). Nonlinear shrinkage estimation of large-dimensional covariance matrices. Annals of Statistics, 40(2), 1024–1060.

Marquand, A. F., Wolfers, T., Mennes, M., Buitelaar, J., & Beckmann, C. F. (2016). Beyond Lumping and Splitting: A Review of Computational Approaches for Stratifying Psychiatric Disorders. Biological Psychiatry: Cognitive Neuroscience and Neuroimaging, 1(5), 433–447.

Mennes, M., Kelly, C., Zuo, X. N., Di Martino, A., Biswal, B. B., Castellanos, F. X., & Milham, M. P. (2010). Inter-individual differences in resting-state functional connectivity predict task-induced BOLD activity. NeuroImage, 50(4), 1690–1701.

Meyer-Lindenberg, A., & Weinberger, D. R. (2006). Intermediate phenotypes and genetic mechanisms of psychiatric disorders. Nature Reviews Neuroscience, 7(10), 818–827.

Nunes, A. S., Peatfield, N., Vakorin, V., & Doesburg, S. M. (2018). Idiosyncratic organization of cortical networks in autism spectrum disorder. NeuroImage.

Oldehinkel, M., Mennes, M., Marquand, A., Charman, T., Tillmann, J., Ecker, C., ... & Buitelaar, J. K. (2019). Archival Report Altered Connectivity Between Cerebellum, Visual, and Sensory-Motor Networks in Autism Spectrum Disorder: Results from the EU-AIMS Longitudinal European Autism Project.

Pruim, R. H., Mennes, M., Buitelaar, J. K., & Beckmann, C. F. (2015). Evaluation of ICA-AROMA and alternative strategies for motion artifact removal in resting state fMRI. NeuroImage, 112, 278–287.

Pruim, R. H., Mennes, M., van Rooij, D., Llera, A., Buitelaar, J. K., & Beckmann, C. F. (2015). ICA-AROMA: A robust ICA-based strategy for removing motion artifacts from fMRI data. NeuroImage, 112, 267–277.

Smith, S. M., Fox, P. T., Miller, K. L., Glahn, D. C., Fox, P. M., Mackay, C. E., ... & Beckmann, C. F. (2009). Correspondence of the brain's functional architecture during activation and rest. Proceedings of the National Academy of Sciences, 106(31), 13040–13045.

van Oort, E. S., Mennes, M., Navarro Schröder, T., Kumar, V. J., Zaragoza Jimenez, N. I., Grodd, W., ... & Beckmann, C. F. (2017). Functional parcellation using time courses of instantaneous connectivity. NeuroImage(November 2016), 1–10.

White, S. J., Coniston, D., Rogers, R., & Frith, U. (2011). Developing the Frith-Happé animations: A quick and objective test of Theory of Mind for adults with

autism. Autism Research, 4(2), 149–154.
Yerys, B. E., Herrington, J. D., Satterthwaite, T. D., Guy, L., Schultz, R. T., & Bassett, D. S. (2017). Globally weaker and topologically different: resting-state connectivity in youth with autism. Molecular Autism, 8(1), 39.